Signature of the Charged Higgs decay $H^{\pm} \rightarrow Wh^0$ With the ATLAS Detector

Kétévi Adiklè Assamagan
Hampton University, Hampton, VA 23668 USA

Abstract

We study the possibility of detecting the charged Higgs through the process $H^{\pm} \rightarrow Wh^0$ with the ATLAS detector. Good reconstructions of the charged Higgs and the neutral Higgs mass peaks are achieved below and above the top-quark mass and the $t\bar{t}$ background is suppressed quite significantly. However, because the expected low signal rates in either region, discovery potential seems limited to a rather narrow area of MSSM parameter space. The results can be normalized to other models, for instance, NMSSM where it is believed there exits quite a range of discovery potential on either side of the top-quark mass.

1 Introduction

The Higgs sector of Minimal Supersymmetric Standard Model (MSSM) contains five physical states, two of which are charged, $H^{\pm}$, and the rest neutral (h^0, H^0, and A^0) [1]. Thus far, the study of the discovery potential of the charged Higgs has concentrated mainly on the fermionic decays modes — $H^{\pm} \rightarrow tb$ and $H^{\pm} \rightarrow \tau\nu$ are the dominant decay channels in most of the parameter space [2]. In the present paper, we study the discovery potential of charged Higgs with the ATLAS detector through the process $H^{\pm} \rightarrow Wh^0$. Though significant only in a tiny range of MSSM parameter space [3], this channel constitutes a unique test for MSSM and is also sensitive to the next-to-minimal extension to MSSM where there may be a significant range of viability on either side of the top-quark mass [4]. The present study is carried out in the framework of PYTHIA5.7 [5] and ATLFAST [6]. In the following sections, we present the details of our analysis below and above the top-quark mass.

2 $H^{\pm} \rightarrow W^{*}h^0$, $m_{H^{\pm}} < m_t$

Below the top-quark mass, we consider $t\bar{t}$ production with one top-quark decaying into W and the other into the charged Higgs. In this case the decay W from the charged Higgs is off the mass shell. The characteristics of the signal is:

$$gg\,(q\bar{q}) \rightarrow t\bar{t} \quad (1)$$

$$t \rightarrow H^{\pm}\, b \quad (2)$$

$$\bar{t} \rightarrow W\, \bar{b} \quad (3)$$

$$H^{\pm} \rightarrow W^{*}\, h^0. \quad (4)$$

Thus, the spectrum contains 2 W's, one of which is off the mass shell, and 4 b-quarks due to the subsequent decay $h^0 \to b\bar{b}$. One of the W's is required to decay into leptons (e, μ) and the other into jets. The major background of this process comes from $t\bar{t}b$ and $t\bar{t}q$ production where both top-quarks decay into W's. Table 1 summarizes the estimated rates for the signal and the background as a function of $\tan\beta$ and $m_{H\pm}$. The results presented in this paper correspond to an integrated

Table 1: The expected rates ($\sigma \times BR$), for the signal $t\bar{t} \to bH^{\pm}Wb$ with $H^{\pm} \to W^{*}h^{0}$, and the $t\bar{t}$ background.

Process	$\tan\beta$	m_{h0}	$m_{H\pm}$	$\sigma \times$ BR (pb)
$H^{\pm} \to W^{*}\,h^{0}$	2.0	83.5	152	1.2
	3.0	93.1	152	0.2
$t\bar{t} \to jjbl\nu b$	2.0			143
	3.0			152

luminosity of 300 fb^{-1} for which we assume a lepton detection efficiency of 90% and a b-tagging efficiency of 50%. A value of the charged Higgs mass smaller that shown in Table 1 results in smaller signal rate as the branching ratio for $H^{\pm} \to Wh^{0}$ drops very rapidly. On the other hand, when $m_{H^{\pm}}$ is closer to the top mass, one of the four b-quarks (mainly the b-quark from $t \to H^{\pm}b$) becomes too soft to satisfy the P_T threshold for b-tagging. In this case, the final state (of either the signal or the background) contains only 3 b-jets and it becomes more difficult to effectively suppress the background. As shown later in the text, the requirement of an extra fourth b-tagged jet, though it reduces both the signal and the background by an additional factor of two, it provides a further suppression of the background by a factor of twenty-five. The data is analyzed as follows:

2-a Search for one isolated lepton (e or μ with $P_T^e > 30$ or $P_T^{\mu} > 6$ GeV/c and $|\eta| < 2.5$), four b-tagged jets (with $P_T^b > 30$ GeV/c and $|\eta| < 2.5$), and at

least 2 non b-jets with $P_T^j > 30$ GeV/c.

2-b At this point, it is not clear which one of the W's decayed into leptons. One is therefore forced to consider the two scenarios:

$$W^* \to l\nu \qquad W \to jj \tag{5}$$

or

$$W^* \to jj \qquad W \to l\nu \tag{6}$$

on event by event basis. A selection is later made based on a chi-square defined below. If the on-shell W decays into leptons, then the W mass constraint is used to fix the longitudinal component P_L^{ν} of the neutrino momentum. This leads, in general, to two solutions. If no physical solution is found, the event is rejected. For this case $W^* \to jj$ and we accept all the jet-jet combinations retained in **2-a**. However, if $W^* \to l\nu$ instead, one can no longer use the W mass constraint. In this case, we set $P_L^{\nu} = 0$ and we retain the jet-jet combinations consistent with the W-mass, i.e., $|m_W - m_{jj}| < 25$.

2-c Consider all the combinations $t_{Wb} \to W b_i$, $h^0 \to b_j b_k$, $H^{\pm} \to h^0 W^*$ and $t_{H^{\pm} b_l} \to H^{\pm} b_l$ for each of the two scenarios in **2-b** and retain the candidate that best minimizes

$$(m_{Wb_i} - m_t)^2 + (m_{H^{\pm}b_l} - m_t)^2. \tag{7}$$

Figure 1 shows the mass reconstructions for the W's as obtained from **2-b** and for the tops as a result of the chi-square selection.

2-d Reconstruct $m_{W^* b_l}$: the signal channel $t_{H^{\pm}b_l} \to W^* h^0 b_l$ is replaced in the background by $t \to W b_l$. Therefore, one would expect $m_{W^* b_l}$ to be consistent with the top mass for the background but not for the signal. Figure 2

shows mass reconstructions for the $W^* b_l$ system, $h^0 \to b\bar{b}$, $t \to H^\pm b$, and $H^\pm \to h^0 W^*$. We retain the event if the following condition is satisfied:

$$|m_{Wb_i} - m_t| < 25 \quad \text{and} \quad |m_{W^* b_l} - m_t| > 50. \tag{8}$$

The improvement in Figure 2 as a result of the cut **2-d** is shown in Figure 3.

2-e Make further cut on $m_{H^\pm b_l}$, i.e., $| < m_{H^\pm b_l} > - m_t| < 50$. The charged and the neutral Higgs mass reconstructions following this cut are shown in Figure 4.

Table 2 lists the efficiency of the cuts **2-a** through **2-e** for the signal and for the background at $\tan\beta = 2.0$. The expected significances and signal-to-background

Table 2: Efficiency of the cuts **2-a**, **2-b**, **2-c**, **2-d** and **2-e**for the signal and the background.

Process	$\tan\beta$	**2-a**	**2-b**	**2-c**	**2-d**	**2-e**
Signal	2.0	2.5%	2.1%	2.1%	1.0%	0.7%
Background		0.14%	0.1%	0.1%	0.03%	$3.4\,10^{-3}$%
S:B		1:4	1:3.4	1:3.4	1:2.7	10:3.6
Signal	3.0	2.7%	2.3%	2.3%	1.1%	0.8%
Background		0.14%	0.1%	0.1%	0.025%	$3.6\,10^{-3}$%
S:B		1:24	1:20	1:20	1:10.7	1:2.1

ratios are shown in Table 3 for $\tan\beta = 2$ and for $\tan\beta = 3$, and for an integrated luminosity of 300 fb^{-1}. This channel presents a significant discovery potential at low $\tan\beta$ (< 2.5) as seen from Figure 4 and Table 3. At high $\tan\beta$, the reconstruction procedure works also well in suppressing the background significantly. From Table 1, for $\tan\beta = 2$, the signal-to-background ratio is worse than 1:100 at the start. The improvement in the suppression of the background is also shown in Table 2; for instance, at $\tan\beta = 2$, the signal-to-background ratio improves to 10:3.6 after all cuts. The difficulty in extracting an observable signal an high

$\tan\beta$ is due mainly to the low signal rate: in fact, as seen in Table 1, the signal rate drops by the factor of six from $\tan\beta = 2$ to $\tan\beta = 3$ while the background remains approximately the same. For an integrated luminosity of 100 fb^{-1}, one

Table 3: The expected signal-to-background ratios and significances for $\mathcal{L} = 3\,10^5$ pb^{-1}.

	$\tan\beta = 2$	$\tan\beta = 3$
m_t (GeV)	192	192
σ_t (GeV)	23	22
$m_{H\pm}$	153	155
$\sigma_{H\pm}$	30	35
m_{h0}	83	93
σ_{h0}	18	17
Signal Events	145	28
Acceptance (%)	83	87.5
$t\bar{t}$ Events	80	125
S/B	1.8	0.22
$S/\sqrt{B}$	16.2	2.5

expects a significance of 9.2 at $\tan\beta = 2$.

In summary, we have studied the discovery potential of the charged Higgs through the decay $H^{\pm} \to W^{*}h^{0}$ for $m_{H^{\pm}} < m_t$. Although the signal rate is two orders of magnitude smaller than the $t\bar{t}$ background rate, we propose a reconstruction procedure which permits the extraction of the signal with a significance exceeding 5σ in the low $\tan\beta(1.5 - 2.5)$ region. At high $\tan\beta$, though the reconstruction is still good, the signal rate decreases so significantly that discovery potential in this region becomes practically nil. In the following section, we examine the situation on the other side of the top mass, i.e., $m_{H^{\pm}} > m_t$.

3 $H^{\pm} \to W h^0, m_{H^{\pm}} > m_t$

Above the top-quark mass, the charged Higgs is produced in association with a top according to:

$$gb \to tH^{\pm} \quad (9)$$

$$H^{\pm} \to Wh^0 \quad (10)$$

$$t \to Wb. \quad (11)$$

The final state for the signal contains 2 W's, one of which decays into leptons, the other into jets, and three b-jets following the decay $h^0 \to b\bar{b}$. The background in this case comes from $t\bar{t}b$, $t\bar{t}q$ and $gb \to tH^{\pm} \to t\bar{t}b$ with both top-quarks decaying into W's. Table 4 shows the signal and the background rates as a function of $\tan\beta$. We assume the same kinematic cuts on η and P_T, and the same efficiencies

Table 4: The rates for the signal $bg \to H^{\pm}t \to Wh^0\,Wb$ and the $t\bar{t}$ background as a function of $\tan\beta$.

Process	$\tan\beta$	m_{h0}	$m_{H\pm}$	$\sigma \times$ BR (pb)
$H^{\pm} \to W\,h^0$	3.0	99.1	200	0.134
	5.0	104.9	200	0.031
$t\bar{t} \to jjbl\nu b$				228

as the in the case $m_{H^{\pm}} < m_t$. The analysis of the data proceeds as described below:

3-a We search for one isolated lepton (e or μ), 3 b-tagged jets, and at least 2 non b-jets satisfying the kinematic conditions stated in **2-a**.

3-b In this case both W's are on-shell and we use the W mass constraint to find a longitudinal component of the neutrino momentum. If no physical solution is found, the event is rejected.

3-c We retain all the jet-jet combinations consistent with the W mass, i.e., $|m_{jj} - m_W| < 25$.

3-d Considering all the $l\nu\, b$ and jjb combinations, the associated top from $gb \to tH^{\pm}$ is reconstructed by minimizing the chi-square

$$\chi^2 = (m_{Wb} - m_t)^2. \tag{12}$$

Figure 5 shows the reconstructions of the W's and the associated top. This procedure not only reconstructs the associated top but it also establishes whether the W selected in the minimization comes from **3-b** or **3-c**. Further, by selecting out one of the b-jets, the minimization process permits the reconstruction of $h^0 \to b\bar{b}$ using the remaining two b-jets in the system. However, the problem of the charged Higgs itself does not present a unique solution: if the selected W from Equation 12 comes from the leptonic channel, $W \to l\nu$, we still have as many charged Higgs candidates as the number of jet-jet combinations retained in **3-c**. On the other hand, if the selected W comes from $W \to jj$, we are, in general, left with two charged Higgs candidates since the neutrino problem **3-b** produces two solutions. For the sake of clarity, henceforth, we refer to the W and the b-jet selected in Equation 12 as W_1 and b_1 respectively, to the remaining W's as W_2, and to the leftover b-jets as b_2 and b_3. The event is accepted for further processing if

$$|m_{W_1 b_1} - m_t| < 25. \tag{13}$$

3-e In order to reduce the number of charged Higgs candidates resulting from **3-d**, $H^{\pm} \to W_2 b_2 b_3$, we reconstruct the invariant masses $m_{W_2 b_2}$ and $m_{W_2 b_3}$ and demand that they must not be consistent with the top mass:

$$|m_{W_2 b_2} - m_t| > 25$$

and

$$|m_{W_2b_3} - m_t| > 25. \tag{14}$$

We show in Figure 6 the combined distributions $m_{W_2b_2}$ and $m_{W_2b_3}$ for the signal and for the background before the condition 14 is imposed. The above requirement suppresses the background further since the background contains an additional top-quark beside the one reconstructed in **3-d**. Figure 7 shows the mass reconstructions for the neutral Higgs, $h^0 \to b\bar{b}$ and for the charged Higgs, $H^{\pm} \to Wh^0$.

Table 5: Efficiency of the cuts **3-a**, **3-b**, **3-c**, **3-d** and **3-e** for the signal and the background.

Process	$\tan\beta$	**3-a**	**3-b**	**3-c**	**3-d**	**3-e**
Signal	3.0	16.9%	12.0%	12.0%	11.5%	4.5%
Background		3.3%	2.3%	2.3%	2.0%	0.8%

The efficiencies of the cuts **3-a** through **3-e** for the signal and the background are shown in Table 5. For an integrated luminosity of 300 fb^{-1}, Table 6 shows the expected signal-to-background ratio and the significance at $\tan\beta = 3$. This channel does not present any discovery potential for the charged Higgs in the range $\tan\beta \geq 3$. This is due the to the low signal rate at the start: from Table 4, the ratio of the signal to background is S:B=1:1700 before any cut is applied. The series of cuts **3-a** to **3-e** improves this ratio to S:B=1:25. However, this is still not enough to observe a clear signature over the background since we can only manage a significance of 2.0 after three years of running at high luminosity.

Table 6: The expected signal-to-background ratio and the significance for $\mathcal{L} = 3\,10^5$ pb^{-1}.

	$\tan\beta = 3$
$m_{H\pm}$	190
$\sigma_{H\pm}$	19
m_{h0}	102
σ_{h0}	24
Signal Events	99
Acceptance (%)	30
$t\bar{t}$ Events	2390
S/B	0.04
$S/\sqrt{B}$	2.0

4 Conclusions

We study the possibility of detecting the charged Higgs through the decay $H^{\pm} \to Wh^0$ with the ATLAS detector. Below the top-quark mass, we consider $t\bar{t}$ production with one of the top-quarks decaying into the charged Higgs, $t \to H^{\pm}b$. The W from the subsequent decay of $H^{\pm}$ is off-shell, $H^{\pm} \to W^*h^0$. We search for a final state containing an isolated lepton, 4 b-tagged jets and at least two non b-jets. This requirement suppresses quite significantly the $t\bar{t}b$ and $t\bar{t}q$ backgrounds. In fact, although the backgrounds are two order of magnitude higher than the signal, the reconstruction technique presented here allows for a significant discovery potential in the low $\tan\beta$ region (1.5-2.5). At higher $\tan\beta$, although the reconstruction is still good, we see no discovery potential because of the much lower signal rates. Above the top-quark mass, the charged Higgs is produced in association with a top-quark, $gb \to tH^{\pm}$. In this case, we search for a final state with an isolated lepton, 3 b-tagged jets and at least two non b-jets. The total background is at least 3 orders of magnitude higher than the signal in the

best case studied, i.e., $\tan\beta = 2$, but with the reconstruction technique presented here, we are able to improve the signal-to-background ratios by two of magnitude. This improvement is still not enough to observe the signal over the background — at $\tan\beta = 2$, we get a significant of 2.0 after 3 years at high luminosity — because of the low signal rates.

In MSSM, the $H^{\pm} \to W h^0$ channel has been excluded by LEP-2 up to $\tan\beta = 3$ because of the non-observation of h^0 [4] [7]. Beyond $\tan\beta = 3$, as demonstrated by the study shown here, this channels presents no discovery potential due to the very low signal rate. It has been argued that in the next-to-minimal extension to MSSM, i.e., NMSSM, this channel is immune to LEP constraints and there may be a significant discovery potential on either side of the top-quark mass [4]. This underscores the main objective of the present study, which is to demonstrate a good signal reconstruction and a high background suppression with the ATLAS detector. The result shown can be normalized to models other than MSSM, including NMSSM, since it is not clear which one to use.

Acknowledgements

The author expresses immense gratitude to E. Richter-Wąs for fruitful discussions and constructive criticisms. The present work is supported by a grant from the USA National Science Foundation (grant number 9722827).

References

[1] P. H. Nilles, *Phys. Rev.* **110**, 1 (1984); H. Haber and G. Kane, *Phys. Rev.* **115**, 75 (1985).

[2] D.H. Miller, S. Moretti, D.P. Roy, and W.J. Stirling, hep-ph/9906230; S. Moretti and D.P. Roy, hep-ph/9909435; K.A. Assamagan, ATLAS Note ATL-PHYS-99-013.

[3] S. Moretti and W.J. Sterling, *Phys. Lett.* **B347** (1995) 291; Erratum, ibidem **B366** (1996) 451.

[4] M. Dress, M. Guchait and D.P. Roy, hep-ph/9909266; and the references therein.

[5] T. Sjöstrand, "High-Energy Physics Event Generation with PYTHIA 5.7 and JETSET 7.4", CERN preprints-TH.7111/93 and CERN-TH.7112/93, Comp. Phys. Comm. **82** (1994) 74.

[6] E. Richter-Wąs, D. Froidevaux and L. Poggioli, ATLAS Internal Note, PHYS-No-079.

[7] R. barate, ALEPH Collaboration, *Phys. Lett.* **B440**, 1998 419. (1996).

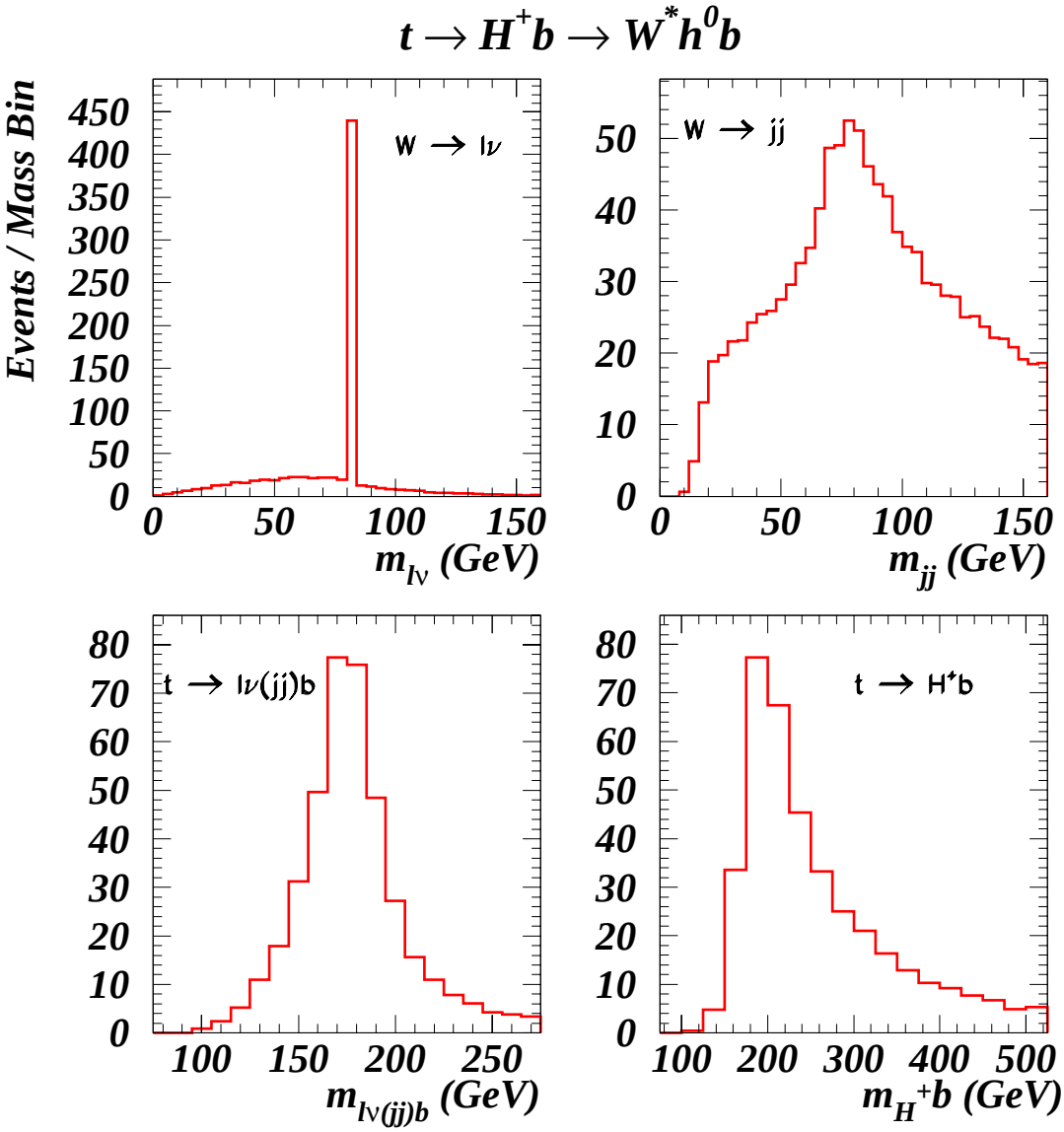

Figure 1: The mass reconstructions for the W's and the top-quarks. The data is shown for signal only and for an integrated luminosity of 300 fb^{-1}.

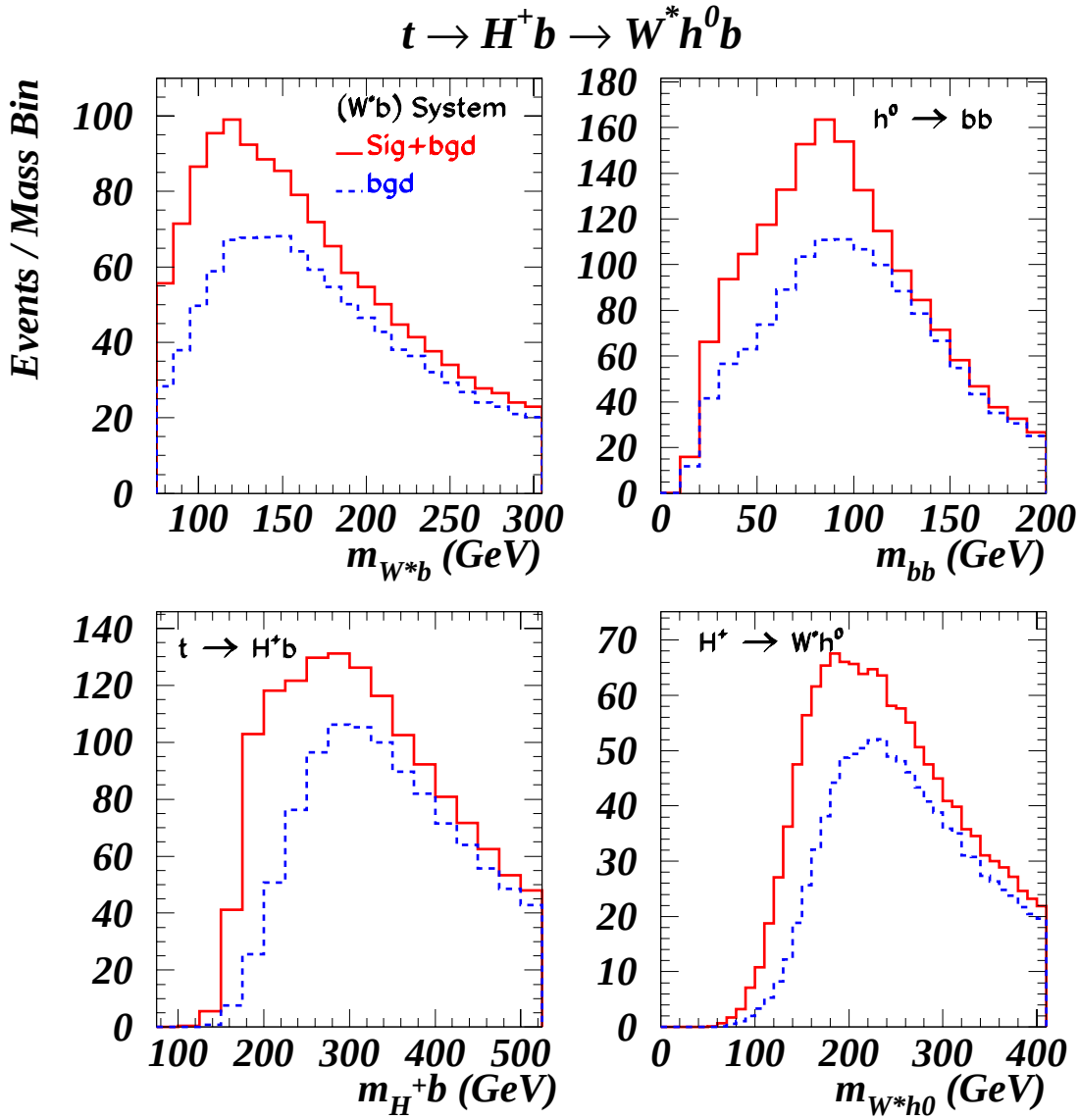

Figure 2: Here, we show the mass reconstructions of the (W^*b) system, $h^0 \to b\bar{b}$, $t \to H^{\pm} b$ and for $H^{\pm} \to W^* h^0$. The data shown is for the combined signal and background, and the background after the chi-square selection, i.e., cut **(c)** and $\tan\beta = 2$.

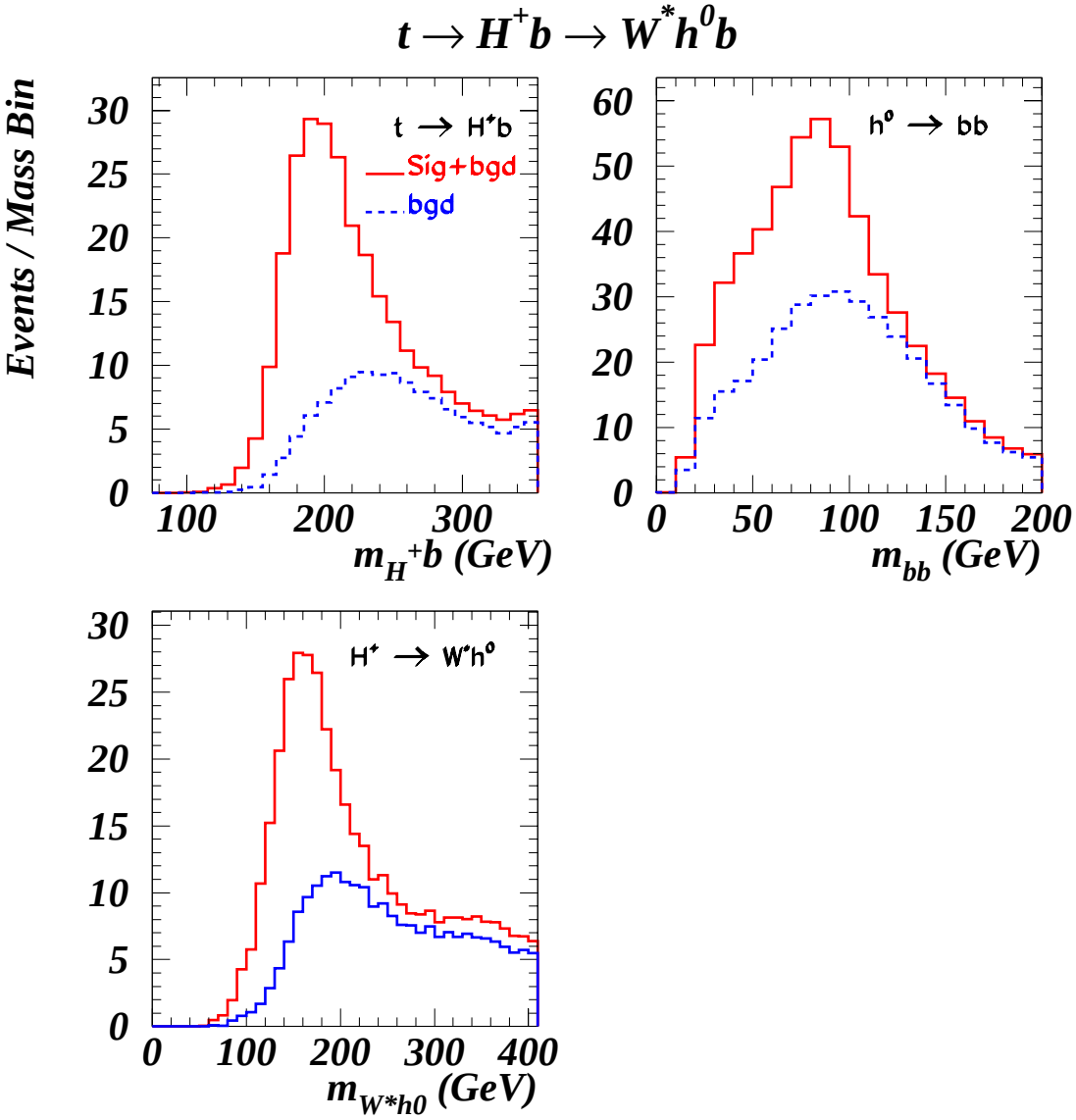

Figure 3: The results after cut **(d)**, i.e., the improvement over the data shown in Figure 2, for $\tan\beta = 2$.

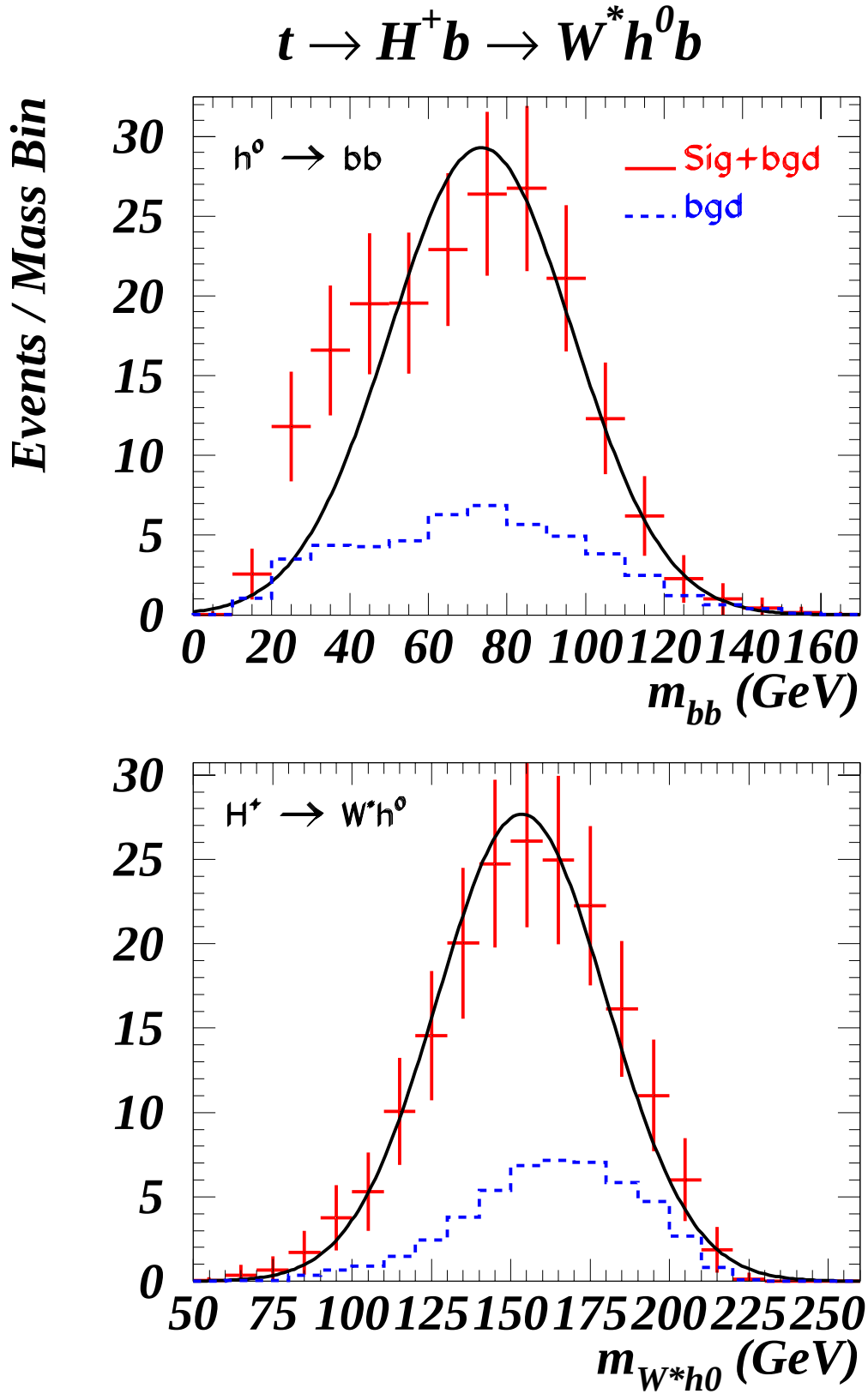

Figure 4: The final mass reconstruction for the neutral and the charged Higgs for $\tan\beta = 2$ after cut **(e)** is applied. The results shown in Table 3 are obtained from this data.

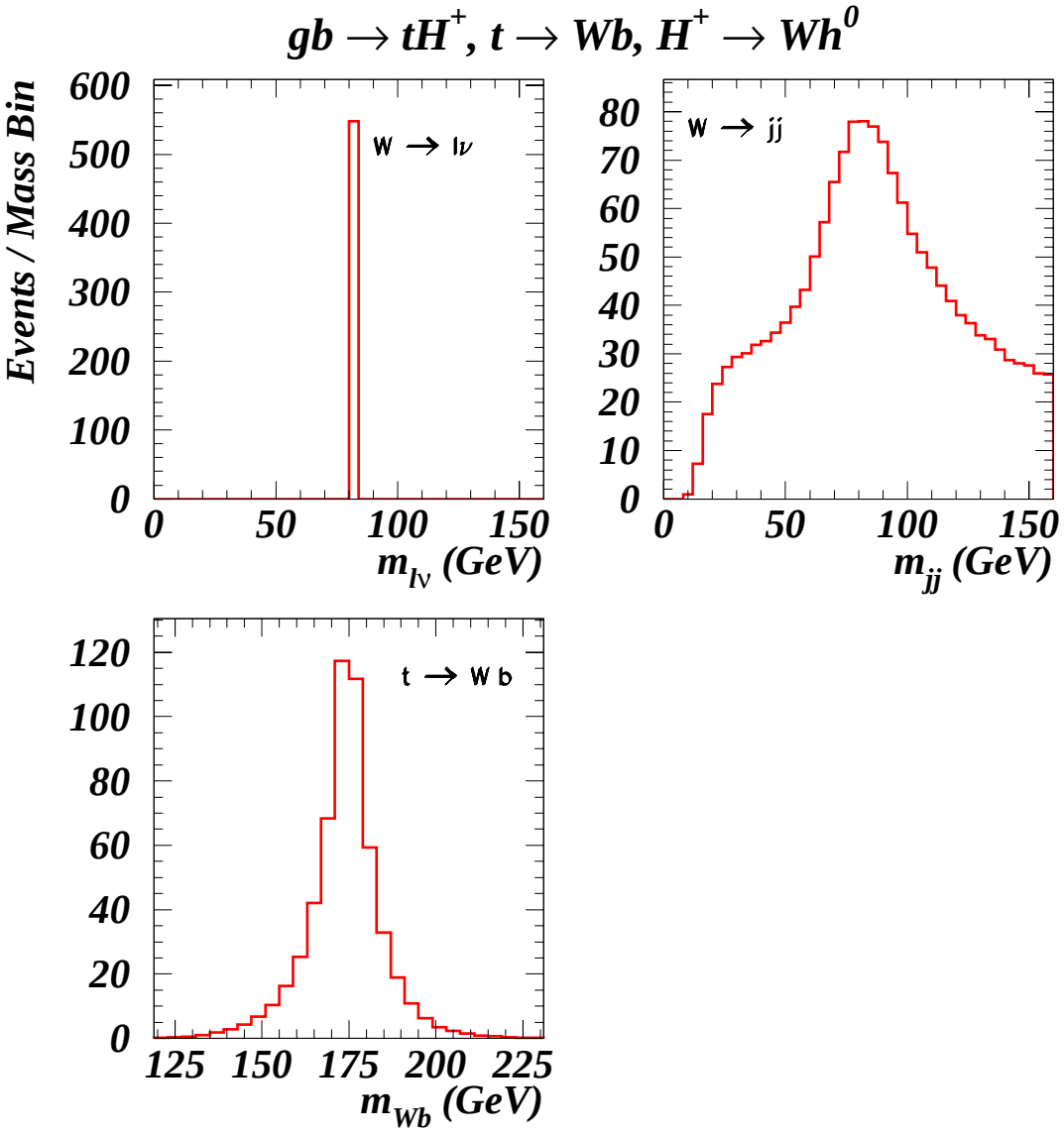

Figure 5: The mass reconstructions for the W's and the associated top for $\tan\beta = 3$ and an integrated luminosity of 300 fb^{-1}. Only the signal is shown.

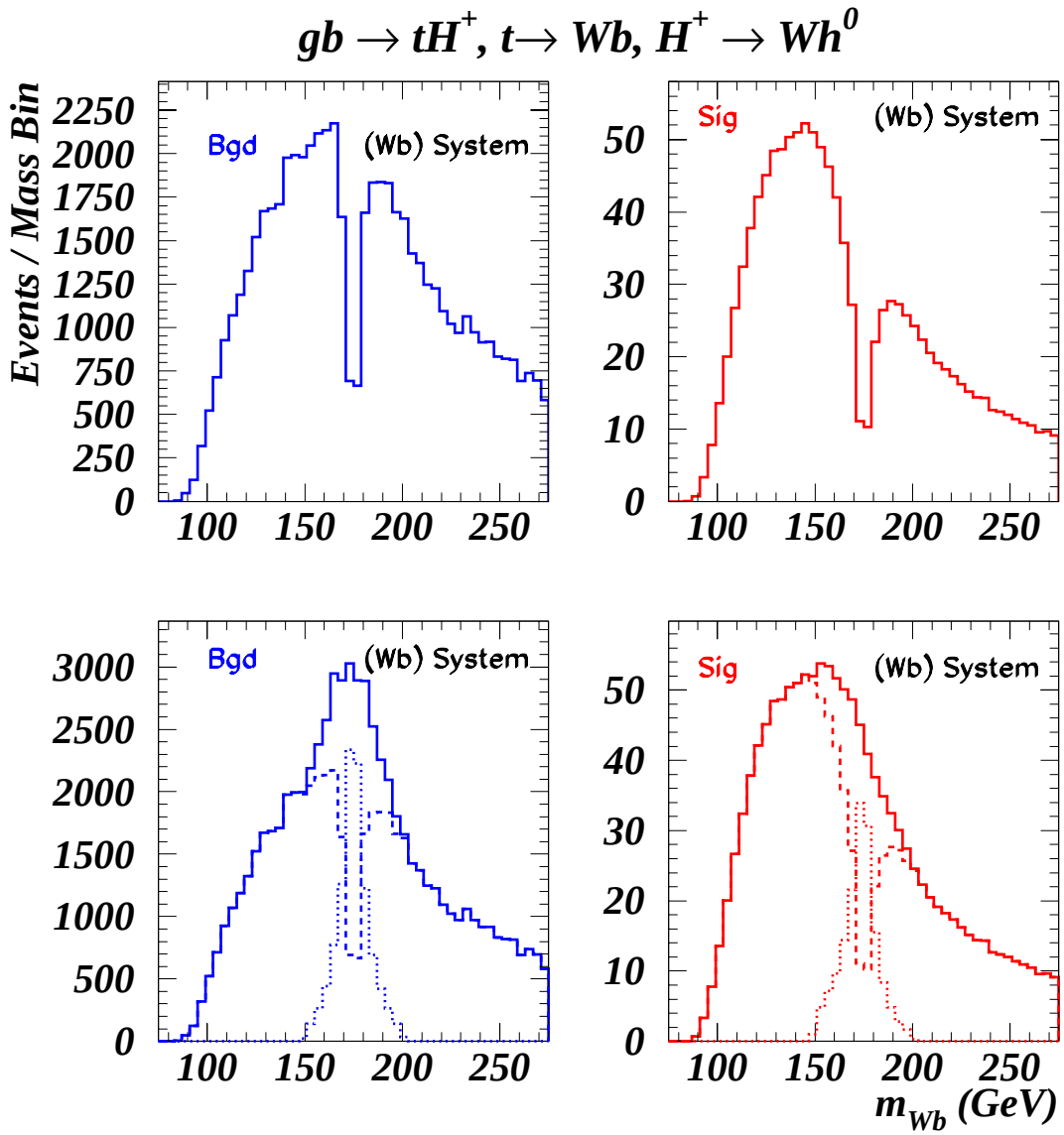

Figure 6: The mass reconstructions for $m_{W_2b_2}$ and $m_{W_2b_3}$ defined in **3-d**. The left panels correspond to the background and the right to the signal. For the background, one expects this distribution to peak at the top-quark mass because of the the additional top-quark in the final state. However, the final state of the signal contains only one top-quark, therefore one does not expect this distribution to peak at the top mass. In the top panels, there is a crack around the top mass. This is due to the misidentification of the correct W and b by the chi-square criterion, Equation 12. In fact, by taking into account the misidentified events, on recovers the full continuous distributions shown in the bottom panels (solid line). In the bottom panels, the dashed line is simply the corresponding top panel and the dotted line is the misidentified W and b combination.

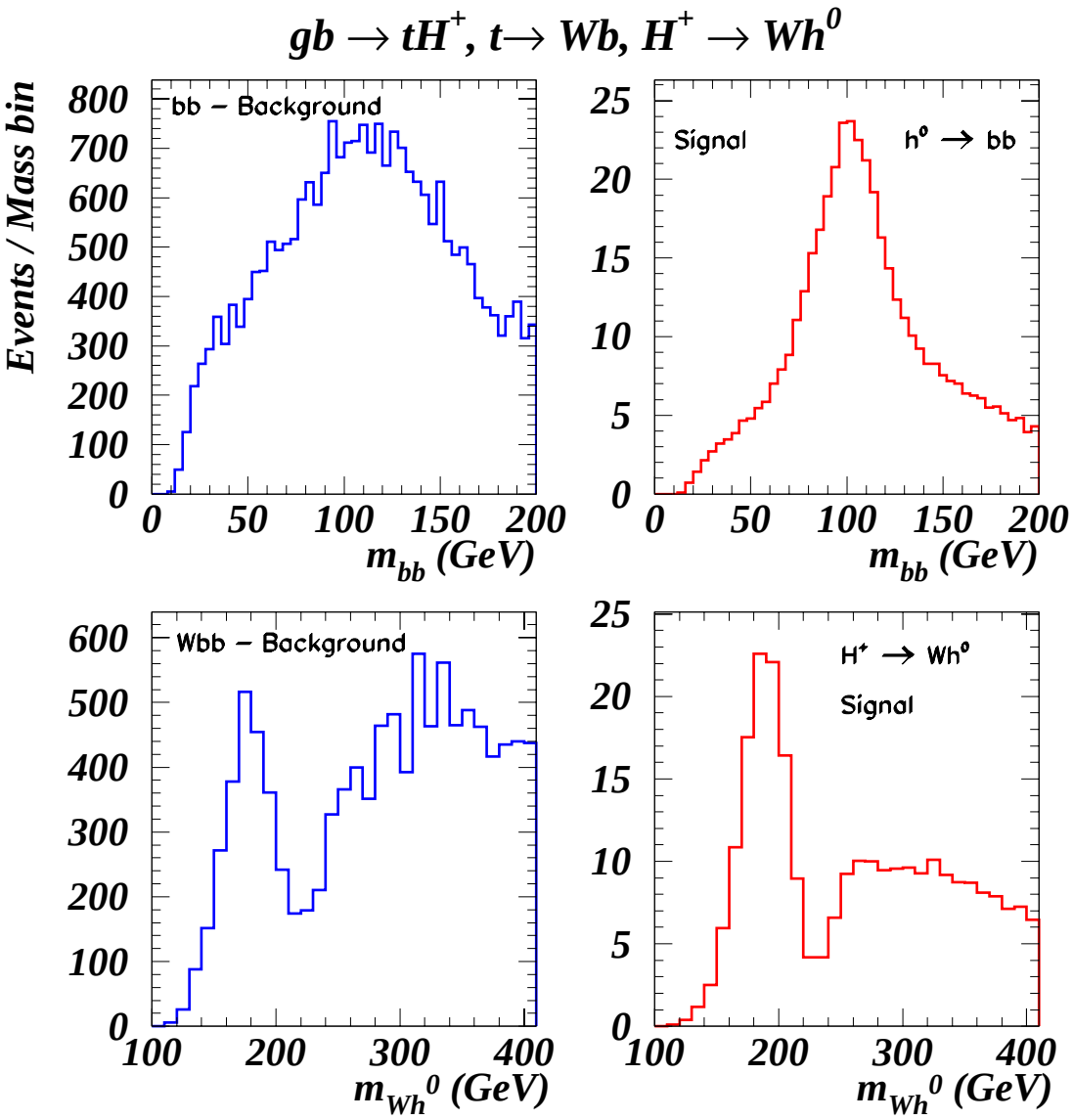

Figure 7: The mass reconstructions for the neutral and the charged Higgs after all the cuts. The results of Table 6 are obtained from this data. The dip in the $m_{H^\pm}$ distributions is due to the cut **3-e**. The m_{bb} distribution for the signal is riding on a combinatorial background.